J Mater Sci (2008) 43:874–882
DOI 10.1007/s10853-007-2152-2

# Computer simulation of carbonitride precipitation during deformation in Nb-Ti microalloyed steels

**Y. Zeng · W. Wang**

Received: 30 October 2006 / Accepted: 10 September 2007 / Published online: 31 October 2007


**Abstract** A thermo/kinetics computer model has been developed to predict the precipitation behavior of complex precipitates in Nb-Ti bearing steels under hot deformation condition. The equilibrium concentration of substitutional elements in austenite and the driving force for precipitation are calculated by the thermodynamic model. The time dependence of volume fraction and mean radius of precipitates is predicted by the kinetics model on the basis of classical nucleation and growth theory. In the kinetics model, the effect of hot deformation on precipitation is taken into account in terms of increase in nucleation sites and the enhanced diffusivity of substitutional solutes along dislocation, the decrease of solute concentration in austenite, and the driving force for precipitation are determined by a mean field approximation method. More importantly, the present model treats nucleation and growth as a concomitant process by using the finite differential method, which is different from the traditional one that treats nucleation and growth as a sequential stage. The model has been further validated by the experimental data in the literature.

## Introduction

High strength, good toughness and improved weldability of HSLA steels can be achieved by the combination of microalloying and controlled rolling. The improvement in mechanical properties results mainly from the refinement of ferrite grain size together with a controlled amount of precipitation strengthening. The microalloying elements such as titanium, niobium and vanadium facilitate grain refinement through precipitation in austenite and contribute to dispersion hardening through precipitation in ferrite. The contributions of titanium, niobium and vanadium to these two processes are significantly influenced by the solubility of their nitrides and carbides in austenite and ferrite. One of the beneficial effects of titanium additions in HSLA steels is an improvement in the weld heat affected zone (HAZ) toughness owing to the stable *Ti*-rich particles formed at high temperature. Niobium can effectively retard the recovery and recrystallization during hot rolling, thus facilitating ferrite grain refinement, whereas vanadium produces less grain refinement but greater dispersion hardening since it has a higher solubility in austenite and precipitates at lower temperatures [1, 2].

Recently, attention has been paid to the combination of *Ti* and *V* or *Ti* and *Nb*, or *Ti*, *Nb* and *V* micro-additions, with the expectation that the potential of each element can be fully exploited. Since the binary carbides and nitrides of *Nb*, *V* and *Ti* are mutually soluble owing to their B1 type structure, this combined addition of metallic elements in steels (multi-microalloying technology) can lead to the formation of compounds with complex chemical compositions [3, 4]; these complex precipitates would further influence the microstructure and mechanical properties of microalloyed steels [5].

Considering the importance of multi-microalloying technology in modifying the microstructure, many experimental attempts and a few mathematical simulations have been made to characterize the complex precipitation behavior in HSLA steels [6–11]. Houghton [9] proposed a thermodynamic model to study the equilibrium solubility and the composition of carbonitrides in *Nb-Ti* bearing austenite on the basis of the Temkin–

Y. Zeng (✉) · W. Wang
Baosteel Technology Center, Shanghai 201900, P.R. China
e-mail: zengyu@baosteel.com

Hillert–Staffansson model. Strid [10] made the first attempt to develop a thermo/kinetic model to simulate particle dissolution kinetics in *Nb-Ti* bearing steel based on Hillert–Staffansson model and Ashby–Easterling model. Okaguchi [11] developed a thermo/kinetics model in the real sense to predict the complex precipitation behavior in *Nb-Ti* bearing steel on a theoretical basis. However, all these models have some deficiencies. For example, Houghton and Strid's model failed to describe the particle precipitation kinetics, and Okaguchi's work ignored the effect of matrix solute concentration and precipitation driving force variation on the precipitation kinetics. Therefore, the present work intends to develop a comprehensive thermo/kinetics model to describe the complex precipitation behavior during hot working in *Nb-Ti* bearing steels. In the thermodynamic part, the equilibrium composition of solute in austenite and the driving force for precipitation are estimated. In the kinetics part, the time dependence of volume fraction and particle radius is predicted considering the influence of concomitant nucleation and growth, solute concentration and driving force variation on the basis of the classical nucleation and growth theory.

## Basic assumptions

Since there are too many factors influencing the precipitation kinetics during hot deformation, it is a very complex work to fully describe the precipitation behavior of carbonitride. In order to simplify the modelling work without influencing the simulation accuracy, the following assumptions are made in our model.

(1) As interstitial atoms diffuse very faster than substitutional atoms in austenite, the kinetics of precipitation is considered to be controlled by the diffusion of substitutional elements *Nb* and *Ti*.
(2) Since the information of dislocation distribution in deformed steels is very difficult to be obtained, we assumed that the dislocations distribute in austenite uniformly.
(3) Precipitates take the form of spherical and their composition can be determined stoichiometrically.
(4) Interfacial compositions between carbonitride and austenite are in local chemical equilibrium.
(5) Since the concentration of *Nb* and *Ti* in austenite is very low, it is considered that the diffusion coefficient of *Nb* and *Ti* is a function of temperature and composition independent.
(6) Substitutional elements (*Nb*, *Ti*) and interstitial elements (*C*, *N*) form ideal dilute solution in complex carbonitrides.

## Thermodynamic calculations

To produce a reliable kinetic model, it is first necessary to have a sufficient understanding of the phase equilibrium of the system being modeled. Thermodynamic calculation for *Fe-M-X* system containing any number of solutes has been developed by a few authors [12–14]. But all these models contain some uncertain parameters, such as solubility product and interaction parameter, and inevitably lead to some calculation error. Gladman's model [15], without any uncertain parameter, can achieve higher calculation precision. Hence, their model was employed to calculate thermodynamic data in our work.

Consider a steel containing A%*Ti*, B%*Nb*, C%*C*, D%*N* (wt%), the basic precipitation reaction for the formation of binary carbides or nitrides in the steel can be written as

$$[M_i] + [X_i] = (M_iX_i) \tag{1a}$$

$$K_i = [M_i][X_i]/a_{M_iX_i} \tag{1b}$$

where $a_{MX}$ represents the activity of the *i*th component, $[M_i]$ denotes the concentration of sustitutional elements in austenite, $[X_i]$ refers to the concentration of interstitial elements in austenite and $(M_iX_i)$ represents the solute concentration in carbonitrides. Considering the formation of a carbide and nitride of titanium and niobium, the following equations are obtained.

$$x[Ti] + (1-x)[Nb] + C = Ti_xNb_{1-x}C \tag{2a}$$

$$y[Ti] + (1-y)[Nb] + N = Ti_yNb_{1-y}N \tag{2b}$$

where $x$ and $y$ are titanium atom fractions in carbide and nitride, respectively. If the above carbide and nitride form a carbonitride phase, then

$$xz[Ti]+z(1-x)[Nb]+z[C]+y(1-z)[Ti]+(1-y)(1-z)[Nb] + (1-z)[N] = Ti_{(xz+y(1-z))}Nb_{((1-x)z+(1-y)(1-z))}C_zN_{1-z}$$

where $z$ is the carbon atom fraction in the carbonitride.

The activities of various components can be described as

$$a_{TiC} = xz \tag{3a}$$

$$a_{NbC} = (1-x)z \tag{3b}$$

$$a_{TiN} = y(1-z) \tag{3c}$$

$$a_{NbN} = (1-y)(1-z) \tag{3d}$$

Substituting the above equations into Eq. 1 provides several equations capable of yielding a complete description of matrix and complex carbonitride as follows.

Define nitrogen concentration in austenite to be [*N*] (wt%), thus nitrogen concentration in the carbonitride can

be written as $D$-[$N$] (wt%), then the matrix compositions can be identified as

$$[Ti] = A - 48(D - [N])(xz + y(1 - z))/(14(1 - z)) \quad (4a)$$

$$[C] = C - 12z(D - [N])/(14(1 - z)) \quad (4b)$$

$$[Nb] = B - 93(D - [N])((1 - x)z + (1 - y)(1 - z))/(14(1 - z)) \quad (4c)$$

Substitute Eqs. 3 and 4 into Eq. 1, we can obtain the following equations.

$$K_1 = \frac{(A - 48(D - [N])(xz + y(1 - z))/(14(1 - z)))(C - 12z(D - [N])/(14(1 - z)))}{xz} \quad (5a)$$

$$K_2 = \frac{B - 93((1 - x)z + (1 - y)(1 - z))(D - [N])/(14(1 - z)))(C - 12z(D - [N]/(14(1 - z)))}{(1 - x)z} \quad (5b)$$

$$K_3 = \frac{(A - 48(D - [N])(xz + y(1 - z))/(14(1 - z)))[N]}{y(1 - z)} \quad (5c)$$

$$K_4 = \frac{B - 93(D - [N])((1 - x)z + (1 - y)(1 - z))/(14(1 - z)))[N]}{(1 - y)(1 - z)} \quad (5d)$$

If Eq. 5c is rearranged to express $y$ in terms of the other variables and $y$ is substituted into Eqs. 5a, 5b, 5d, then the following equations are obtained.

$$x = f_1([N], z)/f_2([N], z) = f_3([N], z)/f_4([N], z) = f_5([N], z)/f_6([N], z)$$

where the six functions are given by

$$f_1([N], z) = A\mathrm{k}_3(1 - z)[C(1 - z) - W]$$
$$f_2([N], z) = z[\mathrm{k}_1(1 - z)(\mathrm{k}_3(1 - z) + Q + 48\mathrm{k}_3 (D - [N])(C(1 - z) - W)/14]$$
$$f_3([N], z) = [((\mathrm{k}_3(1 - z) + Q)(S - B(1 - z) - SA(1 - z)) (C(1 - z) - W]) + k_2 z(1 - z)^2(k_3(1 - z) + S)]$$
$$f_4([N], z) = \mathrm{z}(1 - \mathrm{z})[\mathrm{k}_2\mathrm{k}_3(1 - z)^2 + Q) + 93\mathrm{k}_3(D - [N]) (C(1 - z) - W])/14]$$
$$f_5([N], z) = B[N](1 - z)[\mathrm{k}_3(1 - z) + Q] - [\mathrm{k}_4(1 - z) + S][\mathrm{k}_3(1 - z)^2 + Q - A[N](1 - z)] + z[N](1 - z)(D - [N])[48\mathrm{k}_4/14 - 93\mathrm{k}_3/14]$$
$$f_6([N], z) = z[N](1 - z)(D - [N])[48\mathrm{k}_4/14 - 93\mathrm{k}_3/14]$$

where $S = \frac{93[N](D-[N])}{14}$; $W = \frac{12z(D-[N])}{14}$; $Q = \frac{48[N](D-[N])}{14}$.

Equating any two of the above equations gives three further equations, only two of which are independent. These two independent equations are written as

$$f_1([N], z)/f_2([N], z) = f_3([N], z)/f_4([N], z)$$
$$f_3([N], z)/f_4([N], z) = f_5([N], z)/f_6([N], z)$$

Define two further functions of ([$N$], $z$) as

$$F_1([N], z) = f_1([N], z)f_4([N], z) - f_2([N], z)f_3([N], z)$$
$$F_2([N], z) = f_1([N], z)f_6([N], z) - f_2([N], z)f_5([N], z)$$

Then we have a basis for the numerical (iteration) solution of [$N$] and $z$, with the valid solution satisfying

$$0 < N < [D]$$
$$0 < z < 1$$
$$F_1([N], z) = F_2([N], z) = 0$$

During calculation, the value of $z$ and [$N$] can be determined by an iterative procedure first. Then, the equilibrium concentration of *Nb*, *Ti*, *C*, *N* in austenite and the atom fraction of *Nb*, *Ti*, *C*, *N* in carbonitrides can be obtained by substituting the values of [$N$] and $z$ into the above equations.

## Nucleation

### Nucleation rate

During hot deformation, carbonitrides usually nucleate heterogeneously on dislocations. The steady state nucleation rate $I$ of carbonitride precipitation can be described from the classical nucleation theory as [16]

$$I = N Z\beta \exp\left(-\frac{\Delta G^*}{KT}\right)\exp\left(-\frac{\tau}{t}\right) \quad (6)$$

where $Z$ refers to the Zeldovich non-equilibrium factor, $N$ denotes the number of available nucleation sites per unit volume, $\Delta G^*$ is the critical nucleation energy, $\beta$ represents

the rate of atomic attachment to the critical nuclei, $\tau$ indicates the incubation time and $K$ and $T$ have their usual meanings. It must be noted that there are a range of alternative approaches to calculate $\beta$ and $Z$ on the basis of different assumptions [17–19], and therefore significant differences in the prediction of nucleation rate will be generated. The expression used here was chosen as follows [20].

$$Z = \frac{V_a}{2\pi R^{\bullet 2}}\sqrt{\frac{\sigma}{KT}};\quad \beta = \frac{16\pi\sigma^2 C_M D_{\text{eff}}}{a^4 \Delta G_V^2};\quad \tau = \frac{2KTa^4R^{\bullet 4}}{D_{\text{eff}} V_a C_M \sigma}$$

where $V_a$ is the atom volume of carbonitride, $R^{\bullet}$ is the critical radius, $K$ is the Boltzmann constant, $\sigma$ is the interfacial energy, $a$ is the lattice parameter of austenite, $C_M$ is the average concentration of *Nb* and *Ti* in austenite, $C_M = x.C_M^{Nb} + y.C_M^{Ti}$, where $x$ and $y$ are the atom fraction of *Nb* and *Ti* in precipitates which can be obtained by the thermodynamic model, $C_M^{Nb}$ and $C_M^{Ti}$ are the equilibrium concentration of *Nb* and *Ti* in austenite, respectively. $D_{\text{eff}}$ is the effective diffusion coefficient of *Nb* and *Ti* in austenite and $\Delta G_v$, the volume strain free energy.

Parameter $N$, which represents the number of available sites for heterogeneous nucleation, is assumed to be equal to the number of atoms in the dislocation cores and given as [21]

$$N_{\text{dis}} = N_{\text{hom}} \pi R_{\text{core}}^2 \rho \tag{7}$$

Here, $R_{\text{core}}$ denotes the radius of a dislocation core, $N_{\text{hom}}$ represents the total number of nucleation sites of nucleation within austenite and is expressed as $N_{\text{hom}} = 4/a^3$, $\rho$ is the dislocation density which can be calculated by the method provided in [22].

### Critical nucleation energy and critical radius

During deformation, the overall energy change on forming a spherical nucleation can be given as:

$$\Delta G = \Delta G_{\text{chem}} + \Delta G_{\text{dis}} + \Delta G_{\text{int}} \tag{8}$$

where $\Delta G_{\text{chem}}$ is the chemical free energy and given by $\Delta G_{\text{chem}} = 4/3\pi\ R^{*3}\Delta G_v$, $\Delta G_v$ is calculated using the dilute solution approximation and can be described in terms of compositions as

$$\Delta G_v = RT[\ln\{(X_{Nb0}X_{Ti0}X_{C0}X_{N0})/(X_{Nb}X_{Ti}X_C X_N)\}]/V_P$$

where $X_i$ and $X_{i0}$ are the concentrations of composition $i$ in austenite at temperature $T$ computed by the thermodynamic model and solution temperature, respectively. $V_P$ is the molar volume of precipitates.

$\Delta G_{\text{int}}$ is the interfacial energy between carbonitrides and austenite. The lattice parameter calculation of austenite and carbonitride indicates that for the orientation relation of precipitates, there is about 20% mismatch in lattice spacing. Carbonitrides are therefore expected to be incoherent with austenite, $\Delta G_{\text{int}}$ can be expressed as

$$\Delta G_{\text{int}} = 4\pi R^{\bullet 2} \cdot \sigma$$

$\Delta G_{\text{dis}}$, the strain energy of nucleation of incoherent particles on dislocations, has been studied by Cahn and Gomerez-Ramirez in the situation when the critical radius of a nucleus exceeds the core radius of the dislocation [21, 23]. In fact, on an atomic scale, the diffusion events and relaxation of dislocation line energy associated with nucleation are highly complex. In this work, a simple assumption is made that the core energy of the dislocation line is eliminated over the radius of a nucleus, but the long range elastic strain fields are unaffected. For the estimated core energy of a dislocation line [24], $\Delta G_{\text{int}}$ can be described as

$$\Delta G_{\text{dis}} = 0.4\mu b^2 \cdot R^{\bullet}$$

where $\mu$ is the shear modulus and $b$ is the Burgers vector of the mobile dislocations.

According to Eq. 8, we can obtain the critical nucleation energy $\Delta G^*$ and critical nucleation radius $R^*$ of carbonitride.

## Growth

### Growth rate

The growth of carbonitride is usually considered as a diffusion-controlled growth process. According to Fick's second law, the growth rate can be given by solution of the diffusion equation (Eq. 9) with the following boundary and initial conditions (Eqs. 10a–10c) [25].

$$D\nabla^2 C = \partial C/\partial t \tag{9}$$

$$C(r = R, t) = C_I, \quad 0 < t < \infty \tag{10a}$$

$$C(r = R, 0) = C_M, \quad r \sim R \tag{10b}$$

$$C(r = \infty, t) = C_M, \quad 0 < t < \infty \tag{10c}$$

where $C(r,t)$ denotes the concentration function of position $r$ and time $t$, $D$ represents the diffusion coefficient of substitutional element, $C_I$ refers to the average concentration of *Nb* and *Ti* at the austenite/precipitates interface which is calculated by thermodynamic model.

According to the flux balance law and the invariant field approximation, the growth rate of precipitates is given by

$$g = \frac{\mathrm{dR}}{dt} = \frac{C_M - C_I}{C_p - C_I}\frac{D_{\mathrm{eff}}}{r} \tag{11}$$

where $R$ is the particle radius, $C_P$ is the average concentration of *Nb* and *Ti* in precipitates.

## Diffusion coefficient

Since carbonitrides are nucleated on dislocations during deformation, the precipitates growth is influenced by pipe diffusion along the dislocation core. Therefore, the diffusion coefficient of solute atoms must be an efficient one which takes the influence of both volume diffusion and pipe diffusion into account. In the austenite temperature range and short diffusion time, the volume diffusion depth $L$ ($L = (Dt)^{-0.5}$) of *Nb* and *Ti* is longer than the average distance R($R = \rho^{-0.5}$) among dislocations (assuming $\rho = 10^{14}$/m), then the diffusion coefficient of solute in austenite can be described by Harrison's defects diffusion theory [26] as

$$D_{\mathrm{eff}} = \pi R_{\mathrm{core}}^2 \rho D_{\mathrm{dis}} + \left(1 - \pi R_{\mathrm{core}}^2 \rho\right) D_m \tag{12}$$

where $R_{\mathrm{core}}$ represents the radius of dislocation core, $D_m$ denotes the average diffusivity of *Nb* and *Ti* in austenite, $D_{\mathrm{dis}}$ refers to the average diffusivity of *Nb* and *Ti* along dislocations which can be evaluated from the diffusity in low-angle tilt boundary [27, 28]. $D_m$ and $D_{\mathrm{dis}}$ can be denoted as

$$D_m = xD_m^{Nb} + yD_m^{Ti}$$
$$D_{\mathrm{dis}} = xD_{\mathrm{dis}}^{Nb} + yD_{\mathrm{dis}}^{Ti}$$

where $D_m^i$ and $D_{\mathrm{dis}}^i$ are the diffusion coefficient of element $i$ in austenite and along dislocation line, respectively.

## Variation of matrix concentration and driving force

During the precipitation reaction, the diffusion of substitutional solute atoms into carbonitride will lead to the change of matrix composition, and then influence the subsequent nucleation and growth process. A complex solution for this problem has been suggested by Wert and Zener [29]. For avoiding complexity, Bhadeshia developed the mean field approximation method, which can solve this problem simply without influencing the predicted precision. Hence, this method is used to calculate the averaged concentration of solute in austenite as [30]

$$C_{Mi} = \frac{\left(C_M - V_i C_p\right)}{1 - V_i} \tag{13}$$

where $V_i$ is the real volume of (*TiNb*)(*NC*) phases, $C_{Mi}$ is the modified average composition of solute in austenite.

The driving force will be changed with the variation of solute concentration in matrix. According to Bhadeshia' work, the variation of driving force can be obtained as follows [30]

$$\Delta G_{vi} = (1 - X_\theta)\Delta G_v \tag{14}$$

where $\Delta G_{vi}$ is the chemical driving force at $i$th time step, $X_\theta = V_i/V_{\max}$, where $V_i$ is the instantaneous fraction and $V_{\max}$ is the maximum fraction of a given phase. $V_{\max} = (C_M–C_I)/(C_P–C_I)$.

## Precipitation kinetics

In traditional models, nucleation and growth are treated as a sequential process. In fact, nucleation cannot be finished instantaneously, there must be a process in which nucleation and growth take place concomitantly, and the effect of concomitant nucleation and growth on precipitation kinetics must thus be taken into account for calculation. Therefore, the kinetics of precipitation could be predicted by using the above equations in the following manner.

The thermomechanical process is divided into many time steps. The continuous time evolution of the number and size of precipitates is tracked in terms of discrete time steps. The nucleation rate of new particles and the growth rate of particles nucleated during the preceding time steps are calculated successively; the solute concentration remaining in the matrix and the driving force for precipitation are updated at each time step according to Eqs.13 and 14. Hence, the total particle number $N$ and mean particle radius $\bar{R}$ at time $t$ can be expressed as

$$N = \sum_{i=1}^{n} I_i \quad \bar{R} = \frac{1}{N}\sum_{i=1}^{n} I_i R_i \tag{15}$$

where $I_i$ is the number density of carbonitride precipitated at $i$th time step, $I_i = I\Delta t$, $I$ is the nucleation rate of carbonitride at $i$th time step and $\Delta t$ is the interval of time steps. $R_i$ is the radius of particles nucleated at the $i$th time step, which is given by

$$R_i = R_i^* + \sum_{i=1}^{n} g_i \Delta t \tag{16}$$

where $R_i^*$ is the critical radius of particles nucleated at the $i$th time step and $g_i$ is the growth rate of particles at time $t = i^* \Delta t$.

**Table 1** Parameter values used in calculation

| Symbol | Value | Reference |
|---|---|---|
| $a$ | $3.54 \times 10^{-10}$ m | [19] |
| $V_p$ | $1.3 \times 10^{-5}$m$^3$/mol | [9] |
| $D_{Nb}$ | 0.75 exp(–264000/RT) cm$^2$/s | [9] |
| $D_{Nbdis}$ | 0.75 exp(–204000/RT) cm$^2$/s | [9] |
| $D_{Ti}$ | 0.15 exp(–251000/RT) cm$^2$/s | [9] |
| $D_{Tidis}$ | 0.15 exp(–191000/RT) cm$^2$/s | [26] |
| $R_{\text{core}}$ | $5.0 \times 10^{-10}$ m | [14] |
| $b$ | $2.58 \times 10^{-10}$ m | [14] |
| $\sigma$ | 0.8 J/m$^2$ | [9] |
| $\mu$ | 4.5 Gpa | [14] |
| $V_a$ | $1.90563 \times 10^{-29}$ m$^3$ | |

Then, the total extended volume $\Delta V_e$ at time $i_*\Delta t$ can be expressed as

$$V_e = \frac{4}{3}\pi \sum_{i=1}^{n} (R_i^3 I_i) \tag{17}$$

The widely used Avrami type equation [31] ($X = 1 - \exp(-At^k)$) cannot be applied to the present situation because the equation assumes constant nucleation and growth rates. The generalized KJMA equation [32], which incorporates the temperature and time dependent nucleation and growth kinetics, is applied to the present simulation, and the volume fraction at time $i_* \Delta t$ is thus described as

$$f = 1 - \exp[-V_e] = 1 - \exp[-\frac{4}{3}\pi \sum_{i=1}^{n} (R_i^3 I_i)] \tag{18}$$

The parameter used in calculation is listed in Table 1.

## Calculation results

### Composition in precipitates

The concentration of *Ti*, *Nb*, *C* and *N* in precipitates as a function of temperature was calculated and presented in Fig. 1. It can be seen that the amounts of solute in precipitates decrease gradually with increasing temperature and the dissolution rate of *Nb* is higher than those of other elements. At the temperature ranging from 800 to 1300 °C, the concentration of *Nb* decreases from 0.86 to 0.35%. However, *Ti* content changes only from 0.046 to 0.035%. *N* content decrease very slowly. This result is in agreement with those calculated by other thermodynamic models [10–12]. It can be also found that for steels with this composition, even though the reheated temperature is as high as 1300 °C, there are still some residual carbonitrides in steels, the composition of which is close to the complex nitride, i.e., rich in *Ti* and *N*, depleted in *Nb* and *C*.

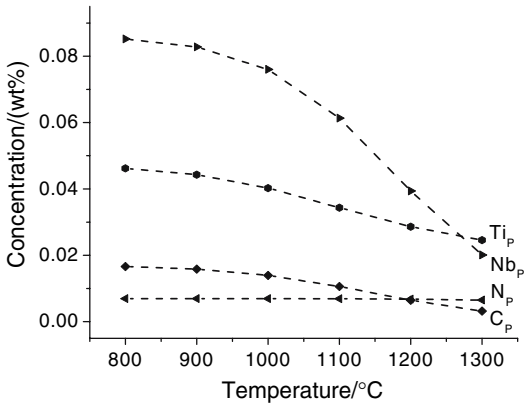


**Fig. 1** The solute concentration in precipitates as a function of temperature in 0.07%*C*–0.007%*N*–0.086%*Nb*–0.047%*Ti* steel, $i_p$ presents the concentration of $i$ element in precipitate

Figure 2 presents the calculated atom fraction change of the elements in precipitates as a function of temperature. It is evident that as temperature increases, the atom fraction of *Ti* and *N* increases and that of *Nb* and *C* value decreases; the precipitates are chemically close to *TiN* gradually. Therefore, *Ti* and *N* are the dominant elements in the quaternary carbonitride at higher temperature.

### Precipitation size and volume fraction

Figure 3 shows the mean radius and volume fraction of precipitates as a function of time at different temperature, respectively. The dislocation density used in calculation is assumed to be $8 \times 10^{14}$ m$^{-3}$. It can be seen from Fig. 5 that at the same temperature, the radius of (*NbTi*)(*CN*) increases with time prelonging. As time approaches 250 s, particles

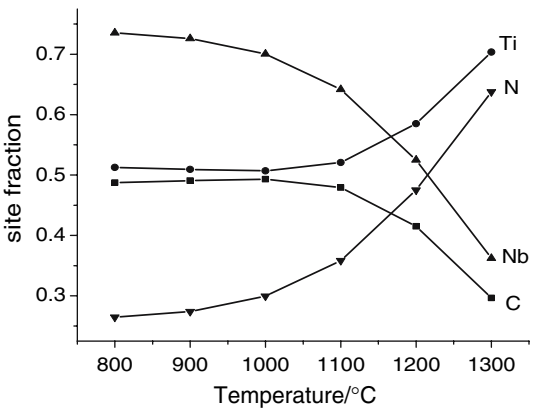


**Fig. 2** The atom fraction of elements in precipitates as a function of temperature in 0.07%*C*–0.007%*N*–0.086%*Nb*–0.047%*Ti* steel

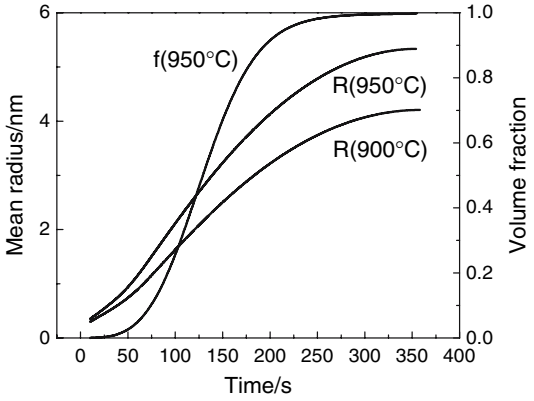


**Fig. 3** Predicted volume fraction and mean radius as a function of time and temperature in 0.1%*C*–0.002*N*%–0.03%*Nb*–0.040%*Ti* steel

grow very slowly because of the exhaustion of solute atoms in austenite. At the same time, as temperature increases, the particle radius increases. The variation of volume fraction with time shows the typical diagram of Avrami equation.

## Nucleation rate and number density

Figure 4 shows the calculated nucleation rate and number density as a function of time at 900 °C in *Nb-Ti* bearing steel. It can be seen that at the initial stage, the nucleation rate increases intensely from 0 to $10^{22}$ $s^{-1}$ $m^{-1}$, and then decreases. When time prolongs to 100 s, the volume fraction precipitated reaches about 30%, the nucleation rate decreases to 0 and the number density of nuclei saturates. This calculation clearly implied that, at the initial stage of precipitation, nucleation and growth take place simultaneously in this steel. After 100 s, nucleation stops and only growth of carbonitrides with different sizes exists in the precipitation process.

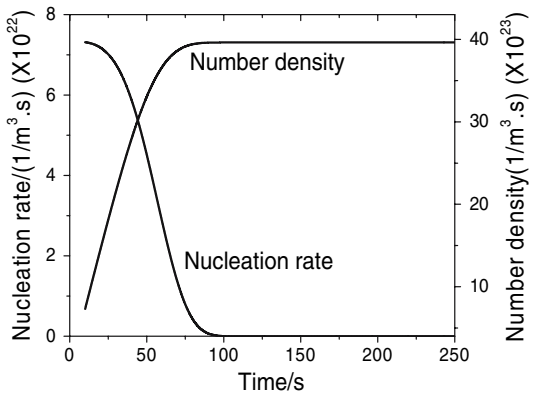


**Fig. 4** The nucleation rate and number density as a function of time at 950 °C in 0.1%*C*–0.002*N*%–0.03%*Nb*–0.040%*Ti* steel

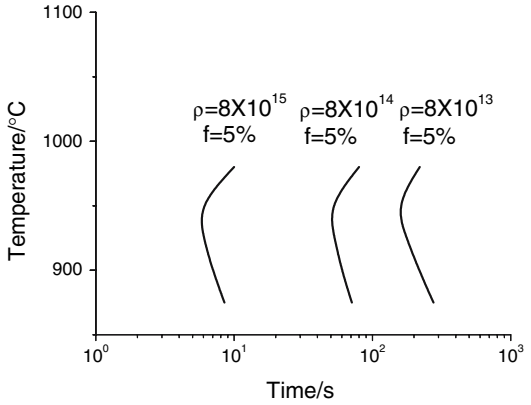


**Fig. 5** The calculated precipitation start curve as a function of dislocation density for 0.1%*C*–0.002*N*%–0.03%*Nb*–0.040%*Ti* steel

## Effect of dislocation density on precipitation

Figure 5 illustrates the precipitation start curve ($f = 5\%$) for 0.1%*C*–0.003*N*%–0.03%*Nb*–0.040%*Ti* steel as a function of dislocation density. It is apparent that when dislocation density is $8 \times 10^{13}$ $m^{-3}$, the precipitation start time corresponding to the nose temperature is about 200 s; when dislocation density increases to $8 \times 10^{15}$ $m^{-3}$, the precipitation start time shortened to about 7 s. This calculation is in good agreement with the experiment data reported in the literature which shows that the presence of dislocations can increase the number of initial nuclei and improve the diffusion coefficient of solute atoms in austenite through pipe diffusion, and then produce a significant acceleration in precipitation kinetics [33, 34].

## Validation of the model

The present model is verified in comparison with a set of published data from literature. Figure 6 shows the comparison between the calculated composition by our thermodynamic model and the microanalyzed composition of precipitates in 0.09%*C*–0.002*N*%–0.027*Nb*–0.063%*Ti* steel reheated at a temperature between 900 and 1250 °C[11]. It can be seen that the calculated value of *Nb*/(*Nb* + *Ti*) ratio ranges from 0.10 to 0.3 with the peak temperature at about 1100 °C in both steels. The calculated *Nb*/(*Nb* + *Ti*) ratio by the present model is in good agreement with the measured one, especially the peak temperature at about 1100 °C in both steels.

Figure 7 is the comparison between the precipitation start time curve calculated by the present model and that of Okaguchi's model in 0.09%*C*–0.002%*N*–0.02%*Nb*–0.042%*Ti* steel [11]. The dislocation density used in calculation is selected from Okaguchi's model. It can be seen that the precipitation curve predicted by both models

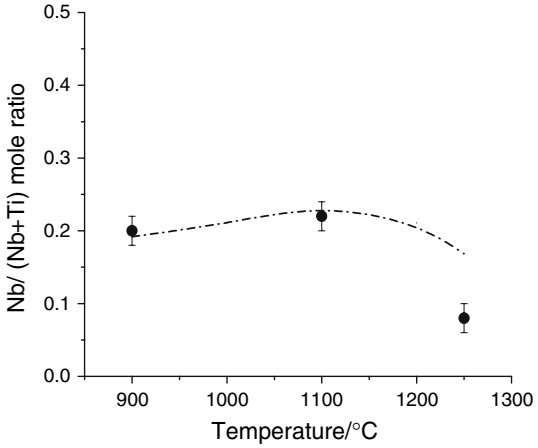


**Fig. 6** Relationship between calculated compositions by the present model and microanalysised composition of precipitates (circled dot) in 0.09%*C*–0.002%*N*–0.027%*Nb*–0.063%*Ti* steel [11]

shows the same typical *C*-curve with a nose temperature at 925 °C, but the precipitation start time calculated by the present model is a little later than that by Okaguchi's model. Validation of the present model with the measured data makes it clear that our model displays a good prediction precision.

Figure 8 illustrates a comparison between the average radius evolution with temperature predicted by the model and the reported data [11]. It can be seen that at the deformation temperature of 900 and 950 °C, the predicted mean radius of precipitates is 4.5 and 6 nm, respectively. Considering the experimental error, we can conclude that the predicted mean radius is in good agreement with the experimental one.

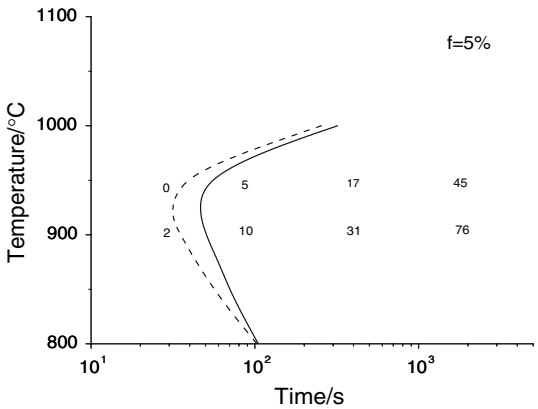


**Fig. 7** Comparison between the predicted start time diagram by the present model and that of okaguchi's model in 0.09%*C*–0.002%*N*–0.02%*Nb*–0.042%*Ti* steel; dashed line shows the precipitation start time curve by Okaguchi's model. The numbers indicate measured fraction of precipitates by Okaguchi [11]

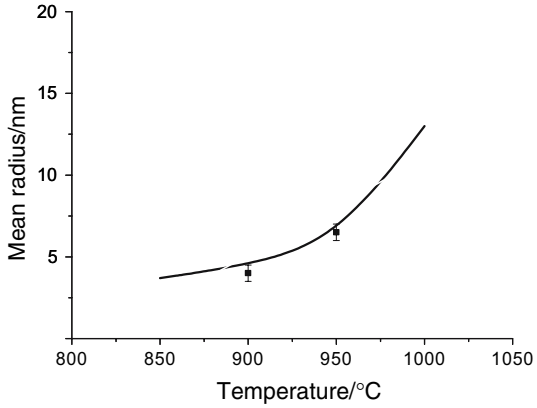


**Fig. 8** Comparison between the predicted mean radius and experimental data [11]; symbol indicates the measured data

## Conclusion

A computer thermo/kinetics model has been developed to predict the complex precipitation behavior in *Nb-Ti* bearing steels on the basis of the chemical thermodynamics and classical nucleation and growth theory. The metallurgical phenomena in the precipitation behavior during hot rolling, such as concomitant nucleation and growth, solute concentration and driving force change, are formulated into the mathematical equations. This model can be used to predict the precipitation kinetics of carbonitride during hot deformation in single *Nb*, *Ti* bearing steel or *Nb* and *Ti* bearing steel. Further work is to build a dislocation density model which considers the effect of recrystallization to further improve the predicted precision of this model.

## References

1. Kanasawa S, Okamoto K (1976) Trans Iron Steel Inst Jpn 16:486
2. Rainforth WM, Sellars CM (2002) Acta Mater 50:735
3. Houghton DH (1982) Thermomechanical processing of microalloyed austenite. AIME, Pennem, p 267
4. Loberg B, Strid J, Easterling KE (1984) Metall Trans 15A:83
5. Okaguchi S, Hashimoto T (1987) Trans Iron Steel Insf Jpn 27:467
6. Hansson P (1989) Scand J Metal 18:295
7. Chen Z, Loretto (1987) Mater Sci Technol 391:836
8. Prikryl M, Kroupa A (1996) Meta Mater Trans 27A:1150
9. Strid J, Easterling KE (1985) Acta Metall 33:2057
10. Heilong Z (1991) Meta Trans 22A:1513
11. Okaguchi S, Hashimoto T (1992) ISIJ Int 32:283
12. Liu WJ, Jonas JJ (1989) Metall Trans 20A:1361
13. Suzuki S, Weatherly C (1987) Acta Metall 18A:211
14. Subramanian SV, Embury JD (1987) Int. Conf on Pipe Technology, Italy
15. Gladman T (1989) The physical metallurgy of microalloyed steels. The Institute of Materials, UK
16. Porter DA, Easterling KE (1992) Phase transformations in metals and alloys. Stanley Thornes, Cheltenham
17. Kashchiev D (2000) Nucleation: basis theory with applications. Butterworth Heinmann, Oxford

18. Kammann R, Wagner R (1991) Mater Sci Tech. Weinheim, VCH
19. Wu DT (1996) In: Solid state physics: advances in research and applications. Academic Press, New York, p 50
20. Robson JD (2003) Acta Metall 23:1453
21. Cahn JW (1957) Acta Metall 51:69
22. Dutta B, Sellars CM (1992) Acta Metal Mater 40:653
23. Gomez-Ramirez R, Pound GM (1973) Metall Trans 7A:1953
24. Weertman JW, Weertman JR (1964) Elementary dislocation theory. Macmillan, New York
25. Aaron HB, Fainstein D (1970) J Appl Phys 41:4404
26. Harrison A (1978) Defects Diffusion Forum 21:576
27. Sutton AP, Balluffi RW (1995) Interface in crystalline materials. Clarendon Press, Oxford
28. Peterson NL (1980) Grain-boundary structure and kinetic. ASM, Metals Park, OH
29. Zener R (1965) J Appl Phys 24:2514
30. Nobuhiro F (2000) Ph.D. thesis, The University of Sheffield
31. Avrami M (1939) J Chem Phys 72:12
32. Kolmogorov AN, Izv A (1937) Nauk Ser Mat 13:55
33. Janampa CS (1982) Ph.D. thesis, The University of Sheffield
34. Liu WJ, Jonas JJ (1989) Metall Trans 20A:689